Supporting Information

Defect-Mediated Electron-Hole Separation on Inorganic-Organic CdS_xSe_{1-x}-DETA Solid Solution under Amine Molecule-Assisted Fabrication and Microwave-Assisted Method for Promoting Photocatalytic H_2 Evolution

Yao Huo[†a], Zhen Li[†a], Jinfeng Zhang[†a], Kai Dai*[a], Changhao Liang*[b], Yangyang[c]

[a] *College of Physics and Electronic Information, Anhui Key Laboratory of Energetic Materials, Huaibei Normal University, Huaibei, 235000, P.R. China.*

[b] *Key Laboratory of Materials Physics and Anhui Key Laboratory of Nanomaterials and Nanotechnology, Institute of Solid State Physics, Hefei Institutes of Physical Science, Chinese Academy of Sciences, Hefei, 230031, P. R. China.*

[c] *Key Laboratory of Microelectronic Devices & Integrated Technology, Institute of Microelectronics, Chinese Academy of Sciences, Beijing 100029, P. R. China*

[†] These authors contributed equally to this work.

* Corresponding authors. Fax: +86-561-3803256

Email address: daikai940@chnu.edu.cn (K. Dai), chliang@issp.ac.cn (C. Liang).

Materials. All chemical reagents (analytical grade) were obtained from Sinopharm Chemical Reagent Co., Ltd., China. Deionized water was obtained an ultra-pure purification system with a conductivity of 18.07 MΩ·cm. All reactants were of analytical purity and used as received without further purification.

Characterization. The crystal structure of inorganic-organic CdS_xSe_{1-x}-DETA hybrid material was investigated by XRD (XRD Rigaku D/MAX 24000). Field emission scanning electron microscopy (FESEM, ZEISS SIGMA 500) and transmission electron microscopy (TEM, JEOL JEM-2100) with an energy dispersive spectrometer (EDS INCA) were employed to investigate the morphologies, structures and element information of the samples. The chemical composition of the samples was determined by XPS (Thermo ESCALAB 250) and Fourier transform infrared (FT-IR NICOLET 6700). Moreover, the UV-Vis diffuse reflectance spectroscopy (DRS) measurements were inspected by PerkinElmer Lambda 950 UV-Vis spectrophotometer. The specific surface area of nanocomposites was investigated by N_2 adsorption data with multipoint Brunauer–Emmett–Teller (BET) method (ASAP2010). The photoelectrochemical measurements were examined by a Shanghai Chenhua CHI-660D electrochemical system. The electrolyte solution was 1.0 M Na_2SO_4. In addition, the 50 mg catalyst was mixed together with 50 μL 5% Nafion and 0.5 mL ethyl alcohol to form the slurry. The slurry was then injected onto a 1.0 cm^2 ITO conductive glass electrode and dried for 30 min at 333 K.

Computational details. In order to investigate the energy band structures of CdS_xSe_{1-x} (x = 0, 0.2, 0.5, 0.8, 1), the density functional theory (DFT) calculations

were carried out by CASTEP code. The generalized gradient approximation (GGA) with Perdew–Burke–Ernzerhof (PBE) form was used as the exchange-correlation function. To establish the model of CdS_xSe_{1-x} of solid solution, the bigger component cation (*i.e.*, the matrix) was replaced by the smaller component cation. The geometry structures of CdS_xSe_{1-x} solid solution models were optimized with the plane wave cutoff of 460 eV and Monkhorst–Pack grids of 3 × 3 × 4 k-points. After geometry optimizations, the band gaps of the CdSe, CdS and CdS_xSe_{1-x} supercells were successfully calculated.

Photocatalytic activity evaluation. The photocatalytic measurement was conducted in a flask with three necks under continuous stirring. A 300 W Xenon lamp (CEL-HXF300, Ceaulight, China) equipped with a UV-cutoff filter ($\lambda \geq 420$ nm) as the light source to drive the photocatalytic reaction. Typically, 50 mg of the photocatalyst was dispersed under stirring in 100 mL aqueous solution of 0.25 M Na_2SO_3 and 0.35 M Na_2S and then bubbled with N_2 to remove the air. The Pt cocatalyst (0.6 wt%) was load onto the surface of photocatalyst by photodeposition method. The distance between the reactor and the Xe lamp is 25 cm. The produced gas was tested by the gas chromatography (Ceaulight GC-7900, TCD). The apparent quantum efficiency (AQE) was calculated according to the following formula:

$$QE[\%] = \frac{number\ of\ reacted\ electrons}{number\ of\ incident\ photos} \times 100\%$$
$$= \frac{number\ of\ evloved\ H_2\ molecules \times 2}{number\ of\ incident\ photos} \times 100\%$$

Table S1 Elemental analyses for $CdS_{0.5}Se_{0.5}$-DETA.

Samples	Atomic ratio analysis of Cd/S/Se by EDS	Atomic ratio analysis of Cd/S/Se by XPS
$CdS_{0.5}Se_{0.5}$-DETA	2.23:0.78:1	2.09:0.81:1

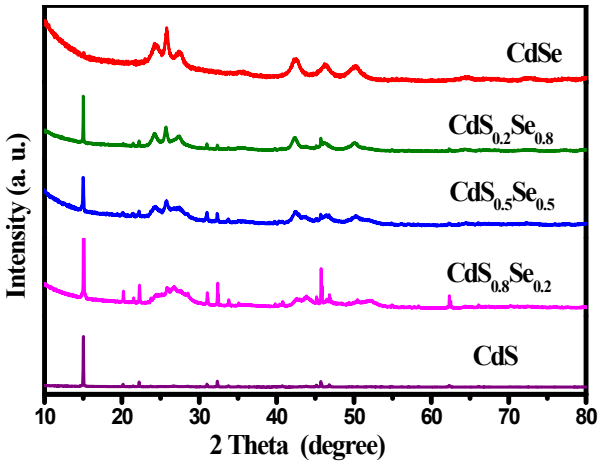

Fig. S1 XRD patterns for CdS_xSe_{1-x}-DETA (x = 0, 0.2, 0.5, 0.8 and 1) without adding DETA.

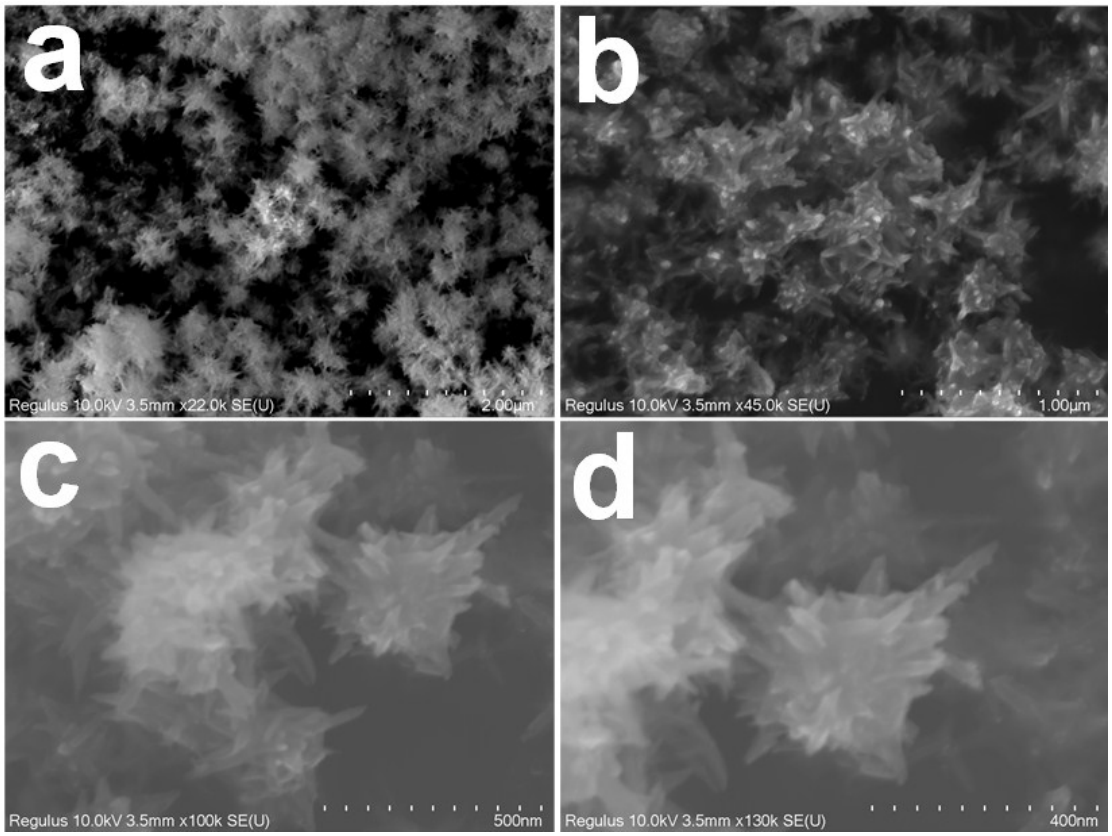

Fig. S2 FESEM images for $CdS_{0.5}Se_{0.5}$-DETA

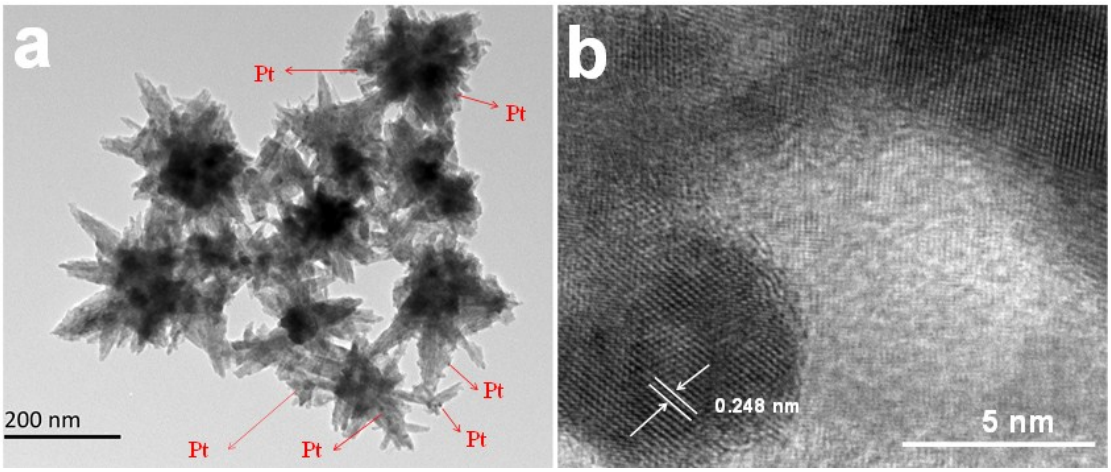

Fig. S3 (a) TEM image and (b) HRTEM image of $CdS_{0.5}Se_{0.5}$-DETA after loading cocatalyst Pt.

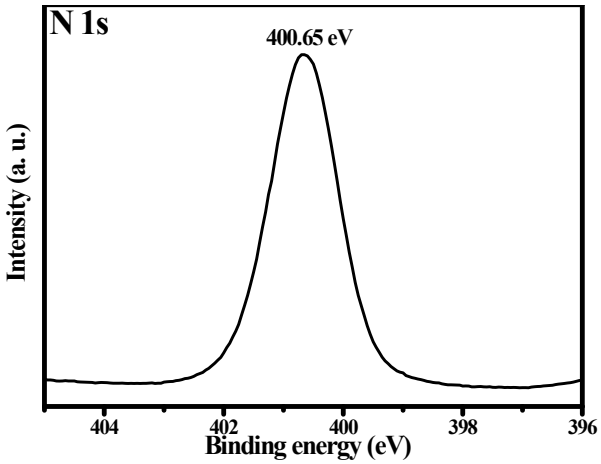

Fig. S4 High-resolution XPS spectra of N 1s for CdS0.5Se0.5-DETA.

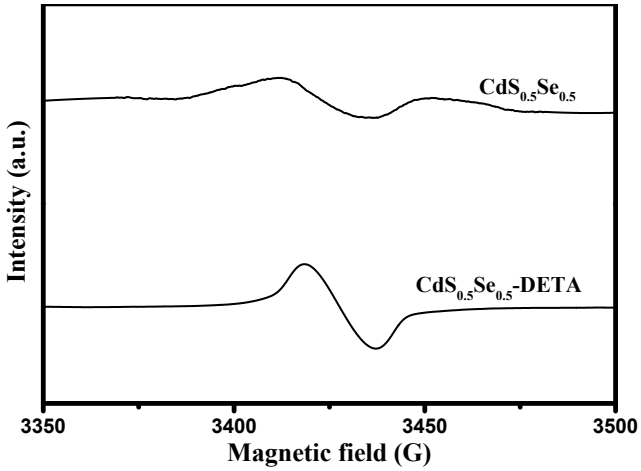

Fig. S5 Room-temperature EPR spectra for $CdS_{0.5}Se_{0.5}$ and $CdS_{0.5}Se_{0.5}$-DETA.

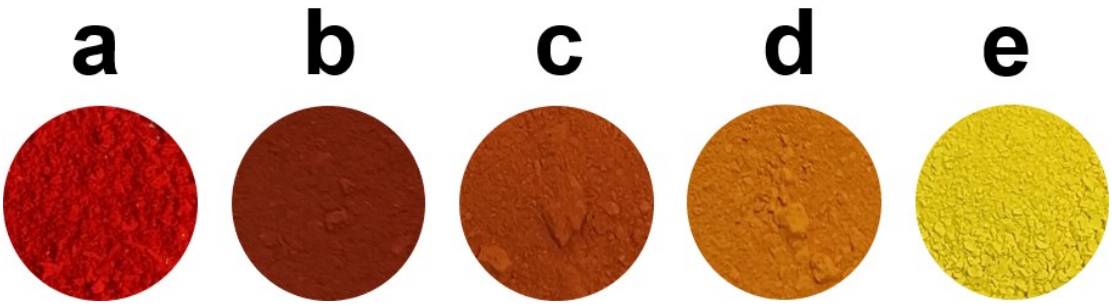

Fig. S6 The color of (a) CdSe-DETA, (b) $CdS_{0.2}Se_{0.8}$-DETA, (c) $CdS_{0.5}Se_{0.5}$-DETA, (d) $CdS_{0.8}Se_{0.2}$-DETA and (e) CdS-DETA.

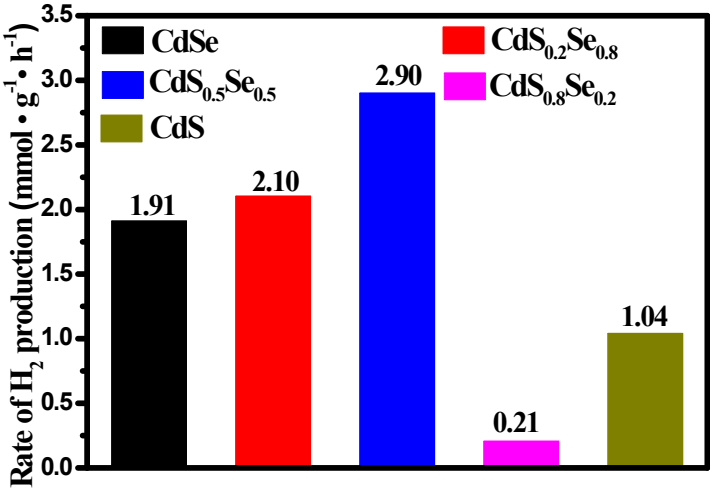

Fig. S7 Comparsion of the photocatalytic H_2-production rates for CdS, CdSe and CdS_xSe_{1-x}.

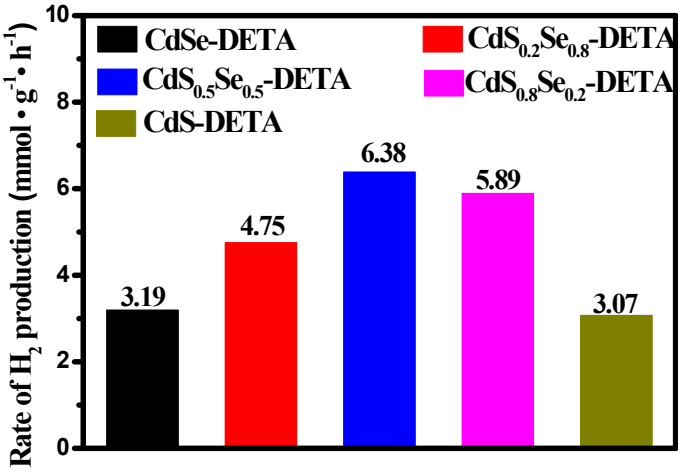

Fig. S8 Photocatalytic H_2-production rates of CdS-DETA, CdSe-DETA and CdS_xSe_{1-x}-DETA without adding Pt cocatalyst.

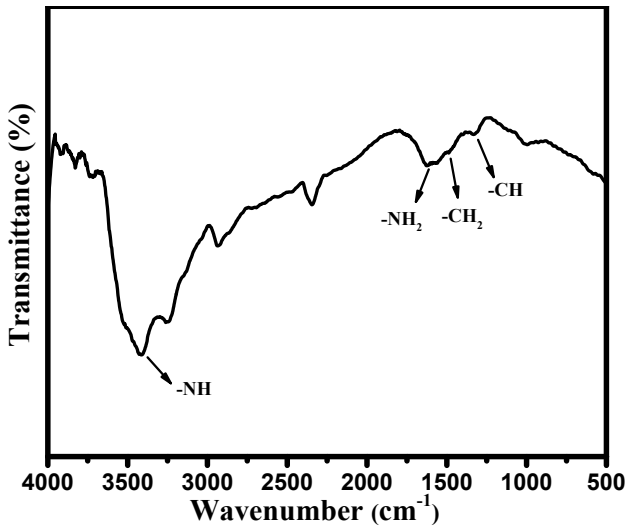

Fig. S9 FT-IR spectra of $CdS_{0.5}Se_{0.5}$-DETA after photocatalytic reaction.